Journal of Physiology (1988), **407**, *pp.* 311–328
With 6 text-figures
Printed in Great Britain

A STUDY OF STRETCH-ACTIVATED CHANNELS IN THE MEMBRANE OF FROG OOCYTES: INTERACTIONS WITH Ca^{2+} IONS

BY VANNI TAGLIETTI AND MAURO TOSELLI

From the Institute of General Physiology, University of Pavia, Via Forlanini 6, I-27100 Pavia, Italy

(*Received 29 March 1988*)

SUMMARY

1. We have carried out patch-clamp measurements on a cationic channel in the plasma membrane of the frog oocyte, which can be specifically activated by membrane stretch. The kinetics of this channel also display a distinct dependence upon membrane potential, the probability of the channel being open increasing with membrane depolarization.

2. When the patch-clamp pipette filling solution was standard Ringer solution, the single-channel current–voltage (I–V) relationship was linear, the elementary conductance being 38 pS and the reversal potential +7 mV, suggesting very poor selectivity of the channel for the various cations.

3. The I–V relationship was highly non-linear having a strong inward-going rectification when Ca^{2+}-free solutions were used to fill the patch pipette. These solutions also resulted in a selective, inward cationic permeability through the membrane, with K^+ being more permeable than $Na^+ > Li^+ > Ba^{2+} > Ca^{2+}$.

4. Though permeant through the stretch-activated channel, Ca^{2+} inhibited in a concentration-dependent manner the currents carried by other cations. La^{3+} (0·1 mM) was also an effective channel blocker.

5. The inward current carried by individual cations at a given membrane potential increased with increasing external cation concentration up to a saturating level, this level being maximal for K^+ and minimal for Ca^{2+}. Also the half-saturating concentration was maximal for K^+ and minimal for Ca^{2+} at all membrane potentials.

6. In the presence of a constant Ca^{2+} concentration (50 μM) increasing $[K^+]$ did not change the absolute level at which the current saturated; however the half-saturating K^+ concentration was greatly increased, indicating competitive inhibition between Ca^{2+} and K^+ for the same site.

7. The data are consistent with a model based on Eyring rate theory for current conduction through ionic channels, in which we assume that the ions capable of entering the channel compete for a binding site that they must first occupy before proceeding on. The possible energy profile of the stretch-activated channel was defined by optimizing the model parameters to obtain the best fit of the experimental data. Ca^{2+} was found to have a smaller dissociation constant and much longer

Authors' names are in alphabetical order.

occupancy time than Na^+ or K^+, thus accounting for its lower permeability and inhibitory effect on current conduction by other cations through the stretch-activatable channel.

INTRODUCTION

An increasing literature has been accumulated during the last years about stretch-activated channels. Unlike voltage- or chemically activated channels, stretch-activated (SA) channels are gated by distortion of the cell membrane. Using the single-channel recording technique, SA channels have been found in chick skeletal muscle (Guharay & Sachs, 1984, 1985), dorsal root ganglion cells (Yang, Guharay & Sachs, 1986), frog lens epithelium (Cooper, Tang, Ree & Eisenberg, 1986), mammalian vascular endothelium (Lansman, Hallam & Rink, 1987), erythrocytes (Hamill, 1983), and *Xenopus* oocytes (Methfessel, Weitzmann, Takahashi, Mishina, Numa & Sakmann, 1986). Recently, SA channels have also been observed in yeast Gustin, Zhou, Martinac, Culbertson & Kung, 1987) and plant cells (Falke, Edwards, Pickard & Misler, 1987). This is not surprising, when considering that these channels may play an important role in cell volume regulation, probably one of the most primitive and essential cell-regulating functions. In the present work, ion conduction in the SA channel of the frog oocyte has been investigated thoroughly, paying particular attention to the ionic selectivity and concentration dependence of single-channel conductance. Briefly, we find that the cations that can enter the channel do not move independently of one another; the Goldman–Hodgkin–Katz equations therefore do not adequately describe the modalities of ion permeation. Conversely, the experimental observations are in agreement with the expectations of a model representing the SA channel as a membrane pore with a single binding site accepting one ion at a time, and displaying different affinities for the various cations. A few observations concerning the open-state probability of the SA channel in relation to applied pressure and membrane potential are also presented.

METHODS

Preparation of oocytes for patch-clamp experiments

All experiments were carried out with oocytes at maturation stages IV–V (Dumont, 1972). Pieces of ovary were removed, after decapitation, from adult females of European frogs (*Rana esculenta L.*) and stored in sterile Barth's medium (mM): NaCl, 88; KCl, 1; $MgSO_4$, 0·82; $Ca(NO_3)_2$, 0·33; $CaCl_2$, 0·41; $NaHCO_3$, 2·4; Tris-HCl, 5; pH 7·4). Penicillin and streptomycin were added at a concentration of 10 μg/ml.

The ovarian epithelium (*theca externa*) and the connective layer (*middle theca*) were mechanically removed with fine forceps. To obtain tight seals of high resistances, the follicular and vitelline envelopes also had to be removed. Our procedure was as follows: following mechanical treatment, the oocytes were incubated with protease (1 mg/ml, type XIV, Sigma) in Barth's medium for few minutes at room temperature, and observed under the dissection microscope. When initial detachment of the vitelline membrane from the cell surface was evident, the oocytes were transferred in Barth's medium containing bovine serum albumin (4 mg/ml, Sigma) and washed several times. The disconnected vitelline membrane was then carefully removed with fine forceps. Using a Pasteur pipette with a wide heat-polished tip, the oocytes were transferred to a tissue-culture dish (Corning 25.000) containing frog Ringer solution (in mM: NaCl, 107; KCl, 2·5; $CaCl_2$, 2; glucose, 5; HEPES–KOH, 10; pH 7·4). In few minutes the oocytes adhered to the chamber bottom.

Patch-current recording

Single-channel current measurements were done at room temperature applying the improved patch-clamp technique in the cell-attached configuration (Hamill, Marty, Neher, Sakmann & Sigworth, 1981), using an L/M EPC-5 (LIST Electronics). The bandwidth of the amplifier was kept at 1 kHz during all measurements. Patch pipettes of 8–10 MΩ resistances were made from borosilicate glass capillaries (Drummond), fire-polished and coated with Sylgard (Dow-Corning, Midland, MI, U.S.A.).

The salt composition of the pipette filling solutions varied in the different experiments, but all contained HEPES (10 mM). The pH was titrated to 7·4 with KOH, NaOH or LiOH (final concentration about 5 mM). Glucose was added to potentially hypotonic solutions to obtain a tonicity of 250 mosM.

After the formation of a high-resistance seal (10–100 GΩ), the membrane patch was stretched by applying suction (i.e. negative pressure) to the patch pipette, using a micrometer-driven syringe connected to a pressure transducer (Godart PAM 58001, DeBilt, Netherlands). Records were taken at different pressures for at least 15 s (90 s in the experiments where the channel open probability was studied), separated by resting periods of 60 s at zero pressure to avoid possible desensitization or slow inactivation of the SA channel. We did not apply pressures greater than 40 cmH_2O, since beyond that value the seals became instable and patch break-down occurred.

The resting potential of the oocytes was determined using a separate intracellular recording electrode filled with 3 M-KCl of 60–100 MΩ resistance and inserted into the oocyte very close to the membrane patch explored. The membrane potentials had mean values around −40 mV ($-42{\cdot}7 \pm 8{\cdot}4$ mV, mean and standard deviation from ninety-four oocytes). Cells with membrane potentials lower than −15 mV were discarded. The actual potential difference across the membrane patch was calculated as the difference between the cell resting potential and the pipette voltage.

Data analysis

Data were recorded on videotape after A–D conversion through a digital audio processor (Sony PCM-701/ES), modified to obtain a bandwidth of 0–20 kHz (Bezanilla, 1985). The analog records were digitized off-line at a sampling frequency of 2 kHz and analysed with a HP 9816 personal computer. Inward currents were represented as upward deflections of the current trace.

The experimental points representing the current–voltage (I–V) and the current–concentration relationships were interpolated with regression functions adjusted to fit the data using standard linear and non-linear regression procedures (Draper & Smith, 1980). Reversal potentials and slope conductances were calculated as the intercept of the voltage axis and the derivative with respect to voltage, respectively, of the best-fitting I–V functions.

Two groups of equations were tested for their ability to predict the experimental observations made with different solutions in the patch pipette: the Goldman–Hodgkin–Katz equations (see for example Hille, 1984), and the equations derived by Lewis & Stevens (1979) for a channel permeable to cations, based on Eyring rate theory for current conduction through ion channels (see for example Hille, 1984). The internal K^+, Na^+ and Cl^- concentrations of the frog oocyte were assumed to be 60, 20 and 50 mM respectively (Taglietti, Tanzi, Romero & Simoncini, 1984). Internal Ca^{2+} concentration was assumed to be negligible.

Single-channel open probability was evaluated as the open probability in each recording (i.e. the total time elapsed in the open state divided by the recording time) divided by the number of channels present in the patch. This was estimated for each experiment as the maximum number of superpositions among single-channel currents, normally occurring at the maximum level of suction applied at the maximum level of membrane depolarization. Due to the somewhat limited range of pressures and potentials investigated here, the actual number of channels present in each patch was probably underestimated.

RESULTS

Pressure and voltage dependence of the stretch-activated channel open probability

An example of unitary currents from a stretch-activated channel in the frog oocyte is shown in Fig. 1*A*. With no suction applied to the patch pipette containing Ca^{2+},

the opening probability was very low and single-channel activity was increased by applying suction through the patch pipette. In preliminary experiments, we observed that a similar activation could also be achieved by applying positive pressures.

More than 90% of the successful patches contained at least one SA channel when the patch pipette was applied to the animal pole of the frog oocyte (we did not explore the vegetal pole). In some patches, channels not sensitive to membrane

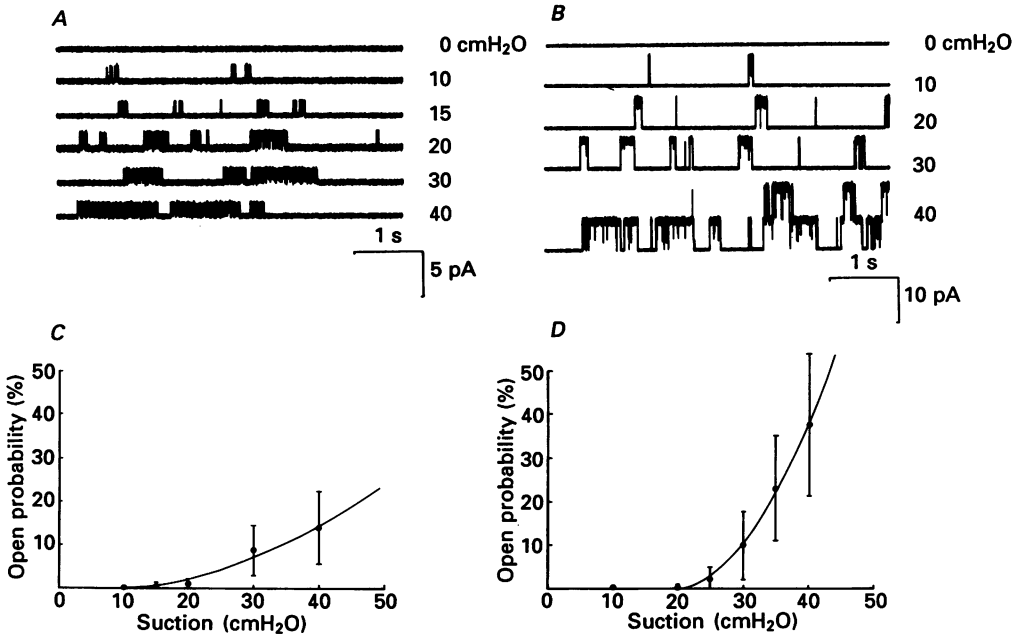

Fig. 1. Pressure dependence of SA channel activity. *A*, sample records with normal Ringer solution in the pipette. The patch membrane potential was kept at −80 mV. *B*, sample records with a 'Ca^{2+}-free' filling solution (in mM: NaCl, 100; EGTA, 10; HEPES–NaOH, 10; pH 7·4). Patch membrane potential, −130 mV. *C* and *D*, open probability plotted *vs.* applied suction in normal Ringer solution (*C*) and with the 'Ca^{2+}-free' solution given in *B* (*D*). Each point is the mean of at least four experiments. The continuous curves are drawn by eye.

stretch were observed; however these could be unequivocally distinguished from the SA channels by their greater current amplitude, smaller open time and negligible opening probability at membrane potentials less than 20–40 mV.

In Fig. 1*B* an example is shown of single-SA-channel activity when Ca^{2+} was absent and EGTA (10 mM) present in the pipette filling solution. Here, the channel displayed marked sensitivity to suction, while open probability increased and channel flickering decreased at pressures greater than 30 cmH_2O.

As shown in Fig. 1*C* and *D*, single-channel probability increased monotonically with increasing negative pressure both in the absence and presence of Ca^{2+}, without any saturation in the pressure range investigated here. Figure 1*D* rules out the possibility that Ca^{2+} ions entering the membrane from outside may represent a step

necessary for activation of the SA channel; mechano-sensitivity is in fact not only maintained, but even augmented with a Ca^{2+}-free solution inside the patch pipette.

The SA channel open probability displays not only dependence upon pressure, but also clear voltage dependence. Examples of SA channel unitary currents at various

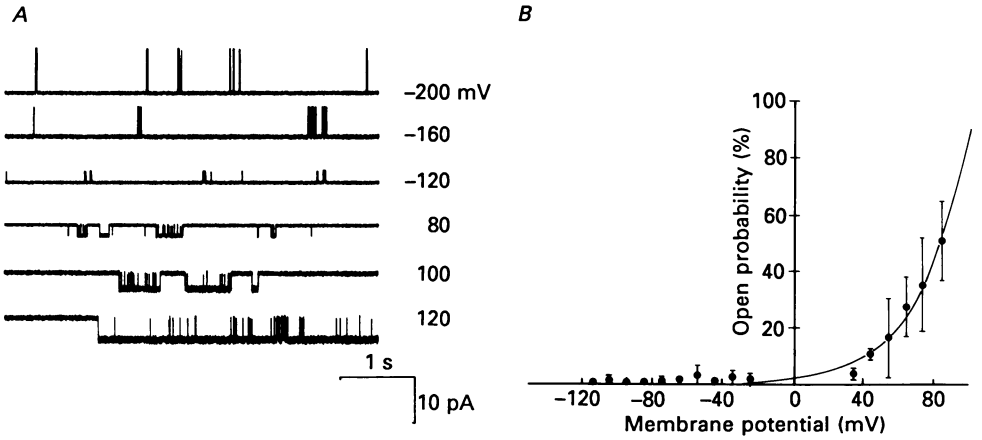

Fig. 2. *A*, sample records showing the voltage dependence of the SA channel activity. *B*, the probability of the channel being open is plotted as a function of patch membrane potential. Pipette filling solution: 100 mM-NaCl, Ca^{2+}-free. Suction applied, 10 cmH_2O. The continuous line is drawn by eye. Each point is the mean of seven experiments.

membrane potentials are shown in Fig. 2*A*. In Fig. 2*B* the single-channel open probability is plotted *vs.* the potential difference across the membrane patch. Open probability is low and practically voltage-independent for negative membrane potentials, but increases sharply at positive potentials.

The kinetics of SA channels will not be analysed in detail in the present paper, which focuses on the dependence, described in the following sections, of the SA channel conductance on voltage and on external ion concentration.

Ionic selectivity and conductance of the stretch-activated channel

The *I–V* relationship using pipette filling solutions of different ionic composition are described first. Figure 3*A* shows the *I–V* relationship with normal Ringer solution.

The different symbols denote four separate experiments in which different degrees of suction were applied. No significant difference was seen between data sets, and we therefore conclude that pressure does not affect the *I–V* relationship of the SA channel. In standard Ringer solution, the single-channel conductance (38 pS) is very close to that reported by Guharay & Sachs (1984) and Cooper *et al.* (1986) with physiological saline (35 and 28 pS respectively).

In the voltage range investigated, the *I–V* relationship was linear with a reversal potential of about +7 mV. This indicates a poor cationic selectivity of the SA

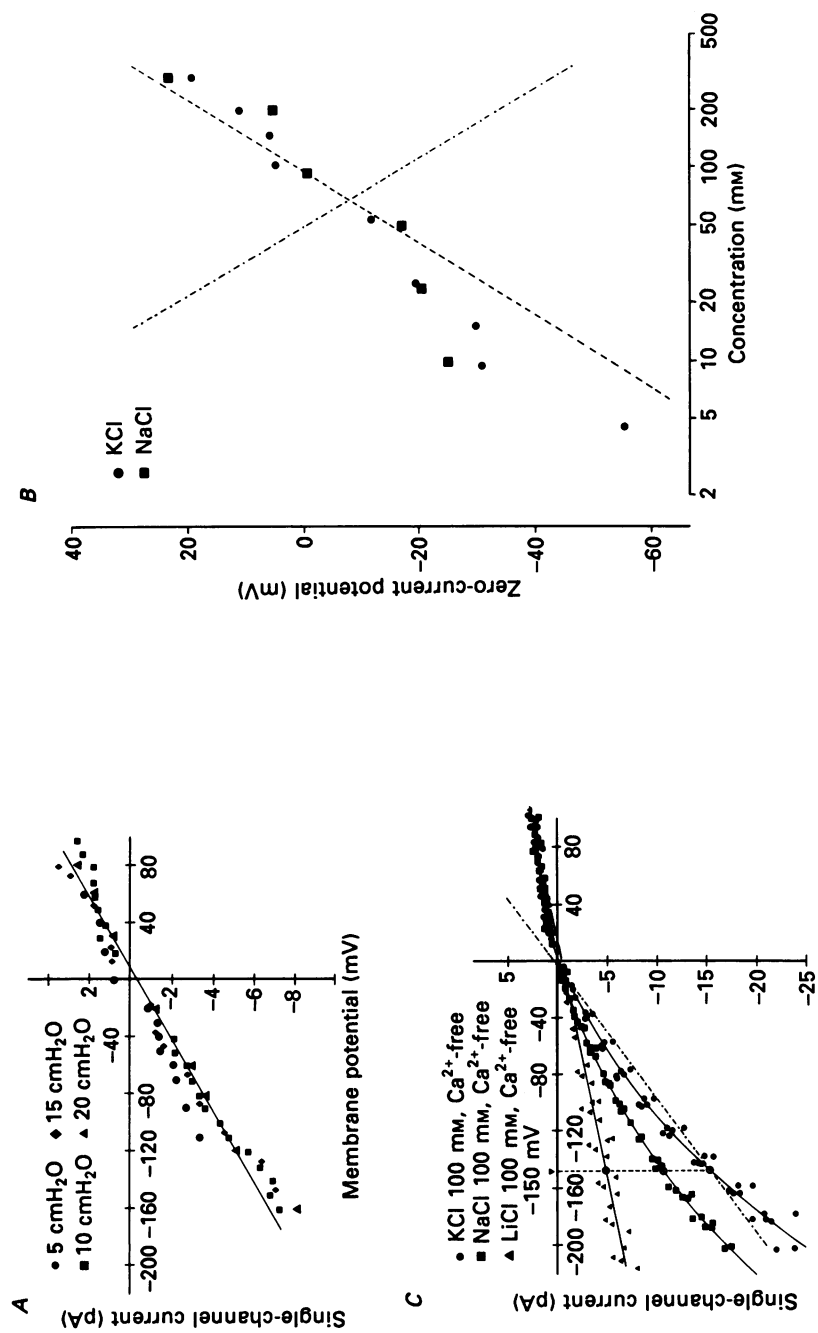

Fig. 3. *A*, current–voltage relationship of the SA channel with normal Ringer solution in the pipette. Different symbols refer to four separate experiments in which different pressures were maintained, as indicated in the inset. *B*, zero-current potentials determined with different concentrations of KCl (●) or NaCl (■), present separately in the filling solution. The dashed line shows the reversal potential predicted by the Goldman–Hodgkin–Katz equation when assuming the channel to be impermeable to Cl^- and $P_{Na}/P_K = 0{\cdot}8$. The dashed–dotted line plots the corresponding Nernst potentials for Cl^-. *C*, *I–V* relationships with the different filling solutions indicated in the inset. The pH was brought to 7·4 using 10 mM-HEPES, buffered with the strong base corresponding to each cation. The dashed–dotted curve is a plot of the current predicted by the Goldman–Hodgkin–Katz equation with a Ca^{2+}-free solution containing KCl (100 mM) filling the patch pipette. The interpolating curves were obtained using standard regression procedures, and the data are from at least four different experiments for each solution.

channel, as E_K and E_{Na} have previously been found to be about -80 and $+40$ mV respectively (Taglietti *et al.* 1984). On the other hand, no statistically significant difference in conductance and zero-current potential was observed when chloride was substituted with an equivalent amount of methanesulphonate in the pipette filling solution. This suggests that the SA channel is impermeable to anions.

The same conclusion could be arrived at from the estimates of the zero-current potentials illustrated in Fig. 3*B*, determined with differing concentrations of either Na^+ or K^+ (no Ca^{2+} was present and 10 mM-EGTA was added). Changing the concentration of K^+ or Na^+ in the range from 5 to 300 mM shifts the zero-current potential between -60 and $+30$ mV. However, a slope of 25·4 mV for an e-fold increase of ion concentration, as expected from the Goldman–Hodgkin–Katz equation for potential, was only obtained in the range 20–300 mM. In this range, the permeability ratio P_{Na}/P_K determined after optimizing the fit of the data to the equation and assuming the internal ion concentrations indicated in Methods, was 0·8 (dashed line). The reversal potentials obviously deviated from the expected trend for low cation concentrations in the pipette filling solution. A possible interpretation is that ion accumulation may occur at the pipette mouth near the outer membrane patch as a consequence of internal cation outflow. At the end, the patch pipette inside is in fact a frustum of a cone having a height of about 20 μm and a mouth diameter of less than 2 μm. If ion electro-diffusion towards the pipette shaft would not occur *ab absurdo*, a current of only 1 pA entering the electrode from the oocyte cytosol would raise in a minute the mean ion concentration in such a narrow volume by about 10 mmol/l. The clearing rate of cations from the outer side of the membrane patch at the pipette tip is difficult to estimate precisely; however a significant accumulation effect could reasonably occur in lower-ionic-strength solutions. The dotted and dashed line drawn in Fig. 3*B* shows the equilibrium potential for Cl^- with various concentrations of NaCl or KCl in the pipette filling solution. It represents the expected zero-current potential if the SA channel were impermeable to cations. The obvious discrepancy between the two lines confirms that the SA channel is a cationic channel impermeable to Cl^-.

However, closer inspection of the *I–V* relationships for Na^+ and K^+ alone (no Ca^{2+}, and EGTA added to the pipette filling solution) revealed that the currents carried in the inward direction by the two cations differed remarkably (Fig. 3*C*). The *I–V* relationship obtained with Li^+ (100 mM) in a Ca^{2+}-free solution is also presented.

In the voltage range explored, the *I–V* relationship was linear when the only monovalent cation present in the filling solution was Li^+. Conversely an inward-going rectification was observed with Na^+ and rectification became even more remarkable with K^+ (note different scales for current axes in Fig. 3*A* and *C*). This rectification does not follow from the independence–constant-field theory; the dashed line in Fig. 3*C* plots the sum of $I_K + I_{Na}$ predicted by the Goldman–Hodgkin–Katz equation for current when K^+ (100 mM) is the only external cation (the ratio P_{Na}/P_K was assumed = 0·8, and $P_K = 2{\cdot}6 \times 10^{-16}$ cm/s to give a total current of $-15{\cdot}9$ pA at -150 mV).

In addition to the apparent rectification, Fig. 3*C* reveals significant selectivity for monovalent cations when they flow inwardly from Ca^{2+}-free solutions. The selectivity sequence is $K^+ > Na^+ > Li^+$. The slope conductances estimated at -150 mV for Li^+, Na^+ and K^+ were $37{\cdot}7 \pm 1{\cdot}8$, $73{\cdot}0 \pm 2{\cdot}3$ and $103{\cdot}9 \pm 5{\cdot}4$ pS, respectively.

Conversely, the unitary outward currents or inward currents at potentials close to E_{rev} were statistically indistinguishable even in Ca^{2+}-free pipette solutions, presumably because, in that potential range, current flow does not depend on the presence and concentration of the external cations, but rather is determined by the (constant) inner ionic composition of the oocyte.

As already mentioned, the plots of Fig. 3*C*, showing rectification and selectivity for inwardly flowing currents, were obtained with Ca^{2+}-free solutions in the patch pipette. When 2 mM-Ca^{2+} was added to the filling solutions containing 100 mM-Na^+ or 100 mM-K^+, both rectification and selectivity disappeared in the voltage range investigated (data not shown), and the respective *I–V* relationships became statistically indistinguishable from those obtained in standard Ringer solution (Fig. 3*A*). In other words, less current flows and no rectification occurs when a few mmol/l of Ca^{2+} are added to pipette filling solutions containing Na^+ or K^+, thus suggesting that Ca^{2+} plays an important role in modifying the SA channel conductance to cations. Below, experiments are described which investigate, first, Ca^{2+} conduction through the channel, and second, the relation between channel conductance to cations and external Ca^{2+} concentration.

The SA channel was permeable to Ca^{2+}, since an inward current was present when the patch pipette contained 75 mM-Ca^{2+} (pH adjusted to 7·4 with 10 mM-HEPES–KOH). To exclude a possible contribution to the inward current by the K^+ ions added to adjust the pH at 7·4 (4·42 mM with 10 mM-HEPES), some experiments were carried out with unbuffered filling solutions (i.e. when only 75 mM-$CaCl_2$ was present in the pipette). No statistically significant difference in the *I–V* relationships was observed in the two sets of experiments. Furthermore, zero-current potentials varied in a range from −20 to 20 mV with varying pipette Ca^{2+} concentrations (10–75 mM, data not shown). When the data were fitted using the Goldman–Hodgkin–Katz equation modified to include the effect of divalent cations on the reversal potential (Fatt & Ginsborg, 1958; Lewis, 1979), the best fit was obtained with a permeability ratio $P_{Ca}/P_K = 1{\cdot}6$.

The *I–V* relationship with 75 mM-Ca^{2+} (buffered with KOH and unbuffered) is shown in Fig. 4*A* and reveals a single-channel conductance of $18{\cdot}5 \pm 1{\cdot}2$ pS. In the same figure we plotted also the *I–V* relationship obtained when Ba^{2+} (75 mM) was present alone in the filling solution: a slight rectification is apparent, and the slope conductance at −150 mV is $37{\cdot}1 \pm 1{\cdot}9$ pS.

Though permeant through the SA channel, Ca^{2+} in the pipette filling solution proved to inhibit the inward flow of Na^+ or K^+ in a concentration-dependent manner. As shown in Fig. 4*B*, for example, the *I–V* relationship obtained with K^+ (100 mM) plus Ca^{2+} (0·05 mM) had a somewhat intermediate position between the *I–V* relationships with the same K^+ concentration and zero Ca^{2+} or 2 mM-Ca^{2+}. Ca^{2+} reduced the single-channel conductance and rectification of inward K^+ or Na^+ currents, and induced channel current flickering (Fig. 4*C*). Ba^{2+} exerted effects similar to Ca^{2+}, though less marked. La^{3+} (100 μM) added to a filling solution containing 100 mM-K^+ completely blocked inward current.

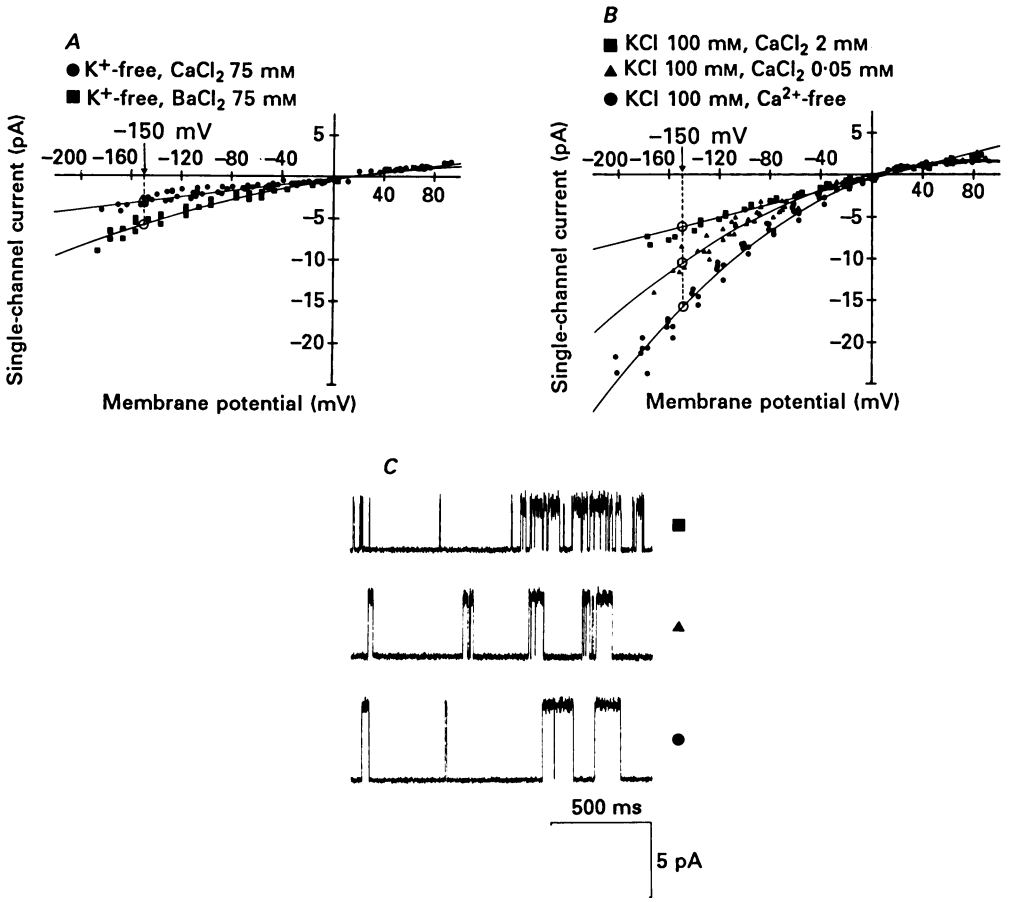

Fig. 4. *A*, *I–V* relationships with filling solutions containing Ca^{2+} or Ba^{2+} (75 mM), as indicated in the inset. The pH was adjusted to 7·4 using HEPES–KOH. *B*, summary of the *I–V* relationships obtained when the K^+ concentration in the pipette was maintained at 100 mM and the Ca^{2+} concentration was raised up to 2 mM. *C*, sample records from the experiments shown in *B*, namely: in the presence of 2 mM-$CaCl_2$ (upper trace), in the presence of 50 μM-$CaCl_2$ (middle trace) and in the absence of Ca^{2+} (lower trace). In all records the membrane potential was −80 mV and the suction applied was between 15 and 25 cmH_2O.

Dependence of current conduction on cation concentration

The data in Fig. 4*B* and *C* suggest that a sort of competitive interaction among cations, in particular between Ca^{2+} and monovalent cations, occurs inside the pore of the SA channel in the frog oocyte. To obtain further information about cation permeation through the channel, the dependence of current flow on external cation concentration was investigated.

In Fig. 5*A* single-channel currents recorded at −150 mV patch membrane potential are plotted *vs.* the concentrations of K^+, Na^+ and Ca^{2+} present separately in the pipette filling solution. Note the current saturation at high cation concentrations.

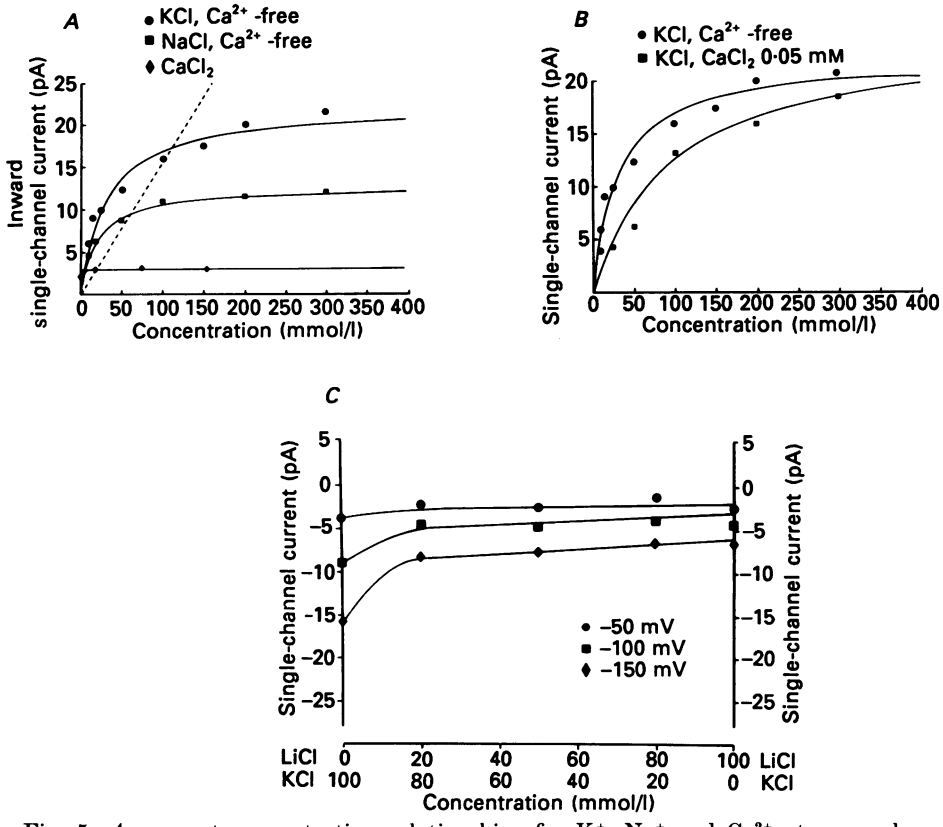

Fig. 5. *A*, current–concentration relationships for K^+, Na^+ and Ca^{2+} at a membrane potential of −150 mV. The data were fitted with a simple Michaelis–Menten saturation function (continuous lines) using standard non-linear regression procedures. The dashed line plots the current–concentration relationship expected for K^+ by applying the Goldman–Hodgkin–Katz equation. *B*, current–concentration relationships obtained with the filling solutions indicated in the inset. *C*, mole fraction experiments using Li^+ and K^+ in Ca^{2+}-free solutions, at the three voltage levels indicated in the inset. The points presented in these plots were calculated from the regression functions best-fitting the experimental data. At least four experiments for each tested solution.

The current–concentration relationships at other membrane potentials also showed a saturation similar to that in Fig. 5*A*. This was not expected from the independence–constant-field theory; the dashed line in the figure plots, for example, the sum of $I_K + I_{Na}$ predicted by the Goldman–Hodgkin–Katz equation for current at −150 mV, when K^+ at varying concentrations is the only cation outside. The experimental points could, however, be fitted, using non-linear regression, to the hyperbola:

$$I_X = \frac{-I_{max,X}}{1+K_{m,X}/[X]_{out}},$$

where $K_{m,X}$ is the half-saturating external concentration of the cation X (Hille, 1984). More experimental points in the range of low ion concentrations would have made

the evaluation of $K_{m,X}$ more precise, particularly for Ca^{2+}. Unfortunately, Fig. 3*B* shows that the data with filling solutions having a very low ionic strength were probably biased by artifact.

The sequences $I_{max,K} > I_{max,Na} > I_{max,Ca}$ and $K_{m,K} > K_{m,Na} > K_{m,Ca}$ shown in Fig. 4*A* were maintained at all potentials, confirming that among these three cations K^+ is able to pass at the highest rate through the SA channel while Ca^{2+} permeates the channel with the greatest difficulty.

TABLE 1. Values of I_{max} and K_m at −150 mV and 0 mV

	−150 mV		0 mV	
Cation	I_{max} (pA)	K_m (mM)	I_{max} (pA)	K_m (mM)
K^+	−22·2	30·8	−11·7	77·2
Na^+	−12·7	20·4	−7·2	53·8
Ca^{2+}	−3·1	0·5	−0·74	1·2

I_{max} and K_m, estimated from current–concentration relations obtained at −150 mV and at 0 mV, are shown in Table 1. I_{max} increased with hyperpolarization as expected due to the increase in driving force; K_m decreased when the membrane patches were hyperpolarized.

In other experiments, K^+ concentration was varied in the patch pipette while Ca^{2+} concentration was maintained at a constant value. In Fig. 5*B*, currents recorded at −150 mV in the presence of 0·05 mM-Ca^{2+} are compared with those recorded in Ca^{2+}-free solutions. The asymptotic value of the current–concentration relation with 0·05 mM-Ca^{2+} (I_{max} = −24·3 pA) was similar to that estimated in the absence of Ca^{2+} (−22·2 pA), but the half-saturating K^+ concentration was much greater ($K_{m,K}$ = 94 mM against 30·8 mM), thus suggesting competitive inhibition between Ca^{2+} and K^+ in the SA channel.

We also performed experiments with various mixtures of monovalent cations inside the patch pipette. Li^+ and K^+ were most interesting because of their remarkably different permeability (Fig. 3*C*). The overall ion concentration inside the pipette was maintained constant at 100 mM as $[Li^+]/[K^+]$ was varied ('mole fraction' experiments). Figure 5*C* shows that the inward currents flowing with various mixtures of monovalent cations in the pipette filling solutions decreased monotonically in amplitude when K^+ was progressively substituted with Li^+. The monotonicity of the current in mole fraction experiments is often taken as evidence that the channel contains only one binding site occupied by the permeating ions moving in single file (Hille, 1984; Almers & McCleskey, 1984).

DISCUSSION

The present data show that the SA channel in the frog oocyte is permeable to cations, and has a selectivity sequence $K^+ > Na^+ > Li^+ > Ba^{2+} > Ca^{2+}$. Although permeant through the channel, external Ca^{2+} reduces the inward current carried by other cations in a concentration-dependent way.

A reasonable interpretation of the above observation is obtained from the experiments where we studied the dependence of the inward current upon the concentration of single-cationic species. The current at a given membrane potential increased with increasing external cation concentration up to a saturating level (I_{max}), as if the various ions capable of entering the channel bind to a saturable site that an ion must first occupy before moving further on. If the half-saturating concentration (K_m) is inversely proportional to the affinity of the permeating ions for the binding site, as assumed from elementary enzyme kinetics, Ca^{2+} should display the maximal affinity, and therefore maximal occupancy time, among the cations tested. Conversely, K^+ should display the minimal affinity and occupancy time. This probably explains why Ca^{2+} permeates the channel with the greatest difficulty while K^+ is able to pass at the highest rate.

Since the presence of Ca^{2+} does not affect the maximal current carried by K^+ at saturating concentrations but increases $K_{m,K}$, it seems reasonable to assume that competitive inhibition between Ca^{2+} and other cations takes place in the SA channel, probably because they bind to the same active site.

The following analysis will formalize this qualitative interpretation.

A possible model for the stretch-activated channel in the frog oocyte

The simple behaviour of the unitary currents as a function of external cation concentration (Fig. 5*A*) and the monotonic variation of the SA current in the mole fraction experiments (Fig. 5*C*) are in agreement with the model of a pore occupied by one ion at a time (Lauger, 1973; Hille, 1975; Urban & Hladky, 1979). Therefore, the most simple physical interpretation of the SA channel in the frog oocyte could be that shown schematically in Fig. 6*A*, comprising a pore with two energy barriers which the cations have to cross to pass through. The energy well between the barriers represents the binding site for the cations within the channel. The energy barriers and well may differ for each type of cation.

The Eyring rate theory for current–voltage relation of ion channels (Eyring & Eyring, 1963; Woodbury, 1971) has been further developed by Lewis & Stevens (1979) for a one-ion channel permeable to cations. Using a similar formalism, the current flowing through the channel can be treated as the rate of the reaction between the various cations (X) present at both sides of the membrane and a charged site inside the channel (S). This reaction may be written for any cation X:

$$X_{out} + S \underset{k_{out,X}}{\overset{f_{out,X}}{\rightleftharpoons}} XS \underset{k_{in,X}}{\overset{f_{in,X}}{\rightleftharpoons}} X_{in} + S. \tag{1}$$

The assumption is made that the binding site must be empty before it can be occupied by any ion. Furthermore, it is assumed that the four hopping rate constants for ion X ($f_{out,X}$ and $f_{in,X}$ for binding, $k_{out,X}$ and $k_{in,X}$ for unbinding) are not affected by the concentration of any other ion in the bathing solutions.

In the Lewis & Stevens (1979) paper, the equation [A 11] for n ions permeating the channel is:

$$I = F\left[\sum_{X=1}^{n} z_X k_{out,X} P(0) \frac{f_{out,X} + f_{in,X}}{k_{out,X} + k_{in,X}} - P(0) \sum_{X=1}^{n} z_X f_{out,X}\right], \tag{2}$$

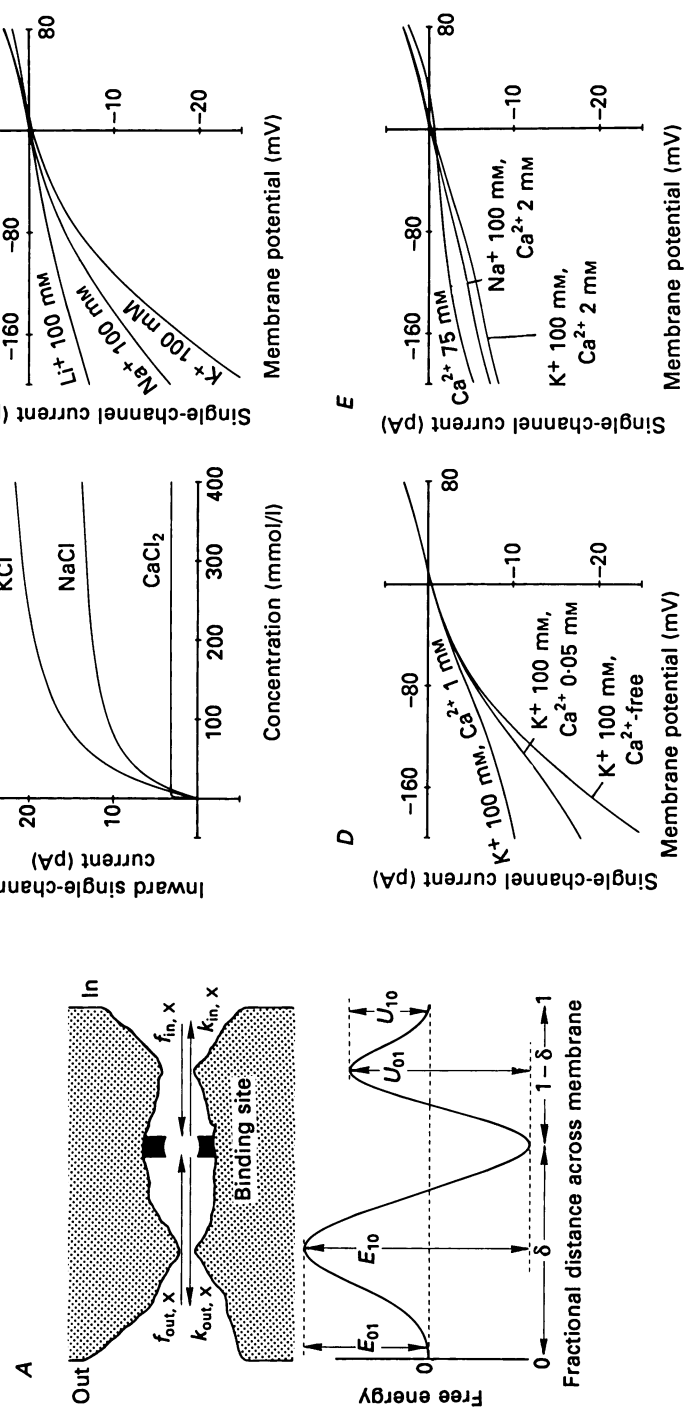

Fig. 6. *A*, hypothetical channel with two barriers and a binding site (upper drawing) and schematic representation of the energy profile inside the channel (lower plot). Reproduced with little modifications from the Fig. 3 by Lewis & Stevens (1979). *B–E*, unitary current amplitudes predicted by the Lewis–Stevens model, using $\delta = 0{\cdot}75$ and rate constants with the voltage-independent components given in Table 2. Each plot simulates the presence of various filling solutions in the patch pipette, indicated by legends. To appreciate the ability of the model to predict the experimental observations, compare the graphs in *B* with Fig. 5*A*, those in *C* with Fig. 3*C*, those in *D* with Fig. 4*B* and those in *E* with Fig. 4*A* and text at p. 318.

where

$$P(0) = \frac{1}{1 + \sum_{X=1}^{n} \frac{f_{out,X} + f_{in,X}}{k_{out,X} + k_{in,X}}}.$$

$P(0)$ is the probability that the binding site is empty and z_X is the valency of the ion X. Each rate constant is then separated into a voltage-dependent term multiplied by a voltage-independent constant denoted by a prime:

$$\begin{aligned} k_{out,X} &= k'_{out,X} \exp(\delta\xi), \\ k_{in,X} &= k'_{in,X} \exp[-(1-\delta)\xi], \\ f_{out,X} &= f'_{out,X}[X]_{out} \exp(-\delta\xi), \\ f_{in,X} &= f'_{in,X}[X]_{in} \exp[(1-\delta)\xi], \end{aligned}$$

where δ is the fraction of the total electrical potential drop across the membrane experienced by the well, $\xi = z_X FV/2RT$ and V is the membrane potential.

To fit all the data with eqn (2) seems a formidable task, since a number of parameters (thirteen) have to be optimized even with $n = 3$, i.e. only considering K^+, Na^+ and Ca^{2+} as permeant cations. However:

(a) The unbinding rate constants $k_{in,X}$ can be calculated from the maximum inward current I_{max} carried at a given membrane potential by each ion at saturating external concentration. The simple limit of eqn (2) is in fact, for an infinite external concentration of the X ion,

$$I_{max,X} = -z_X e k_{in,X},$$

where e ($1{\cdot}6 \times 10^{-19}$ C) is the absolute electrical charge carried by one electron and z is the ion valency. $k_{in,X}$ is expected to exponentially increase with hyperpolarization; however its voltage-independent component $k'_{in,X}$ can be calculated from $I_{max,X}$ at zero membrane potential. Data in Table 1 give $k'_{in,X} = 7{\cdot}3 \times 10^7\ s^{-1}$, $k'_{in,Na} = 4{\cdot}5 \times 10^7\ s^{-1}$ and $k'_{in,Ca} = 2{\cdot}3 \times 10^6\ s^{-1}$, respectively.

(b) The permeability ratios $P_{Na}/P_K = 0{\cdot}8$ and $P_{Ca}/P_K = 1{\cdot}6$ give the ratios of the binding rate constants for Na^+ and Ca^{2+} $f'_{out,Na}/f'_{out,K}$ and $f'_{out,Ca}/f'_{out,K}$ relative to K^+ in the absence of electrical field.

(c) At zero potential, $U_{01} - E_{10} = U_{10} - E_{01}$, and the voltage-independent components of the four rate constants are related by the simple relation:

$$\frac{k'_{out,X}}{k'_{in,X}} = \frac{f'_{out,X}}{f'_{in,X}}.$$

(d) By placing the energy well half of the electrical distance through the membrane ($\delta = 0{\cdot}5$), as is often done for simplicity in modelling one-ion channels, the model predicts substantial inward rectification which is more marked for divalent than for monovalent cations. Conversely, the SA channel gave I–V relationships with Ca^{2+} which looked linear (Fig. 4*A*), whereas the I–V relationships with K^+ and Na^+ alone (Fig. 3*C*) strongly rectified. Shifting the energy well towards the inner membrane side substantially reduced rectification for inward currents, but much more remarkably for divalent than for monovalent cations. We assumed $\delta = 0{\cdot}75$, since this value made negligible the rectification expected with Ca^{2+} in the voltage range investigated while it left rectification with Na^+ or K^+ similar to that observed.

These restrictions leave three parameters to be optimized in eqn (2) ($f_{out,K}$, $f_{in,K}$ and $f_{in,Na}$), if $f_{in,Ca}$ is assumed to be negligible for the internal Ca^{2+} concentration. The values of the voltage-independent component of the four rate constants for each ion producing the best fit of all the results of the present work are shown in Table 2, along with the heights of the corresponding energy barriers in the absence of an electrical field across the membrane. Notice that the binding rate constants for the three cations are of the same order of magnitude, whereas we obtained unbinding rate constants for Na^+ and K^+ more than tenfold greater than those for Ca^{2+}.

TABLE 2. The rate constants are given in s^{-1}; the heights of the corresponding energy barrier at zero potential are given as reduced free energies, i.e. in *RT* units. Multiply by 2·45 to obtain the actual activation energies required to pass over each barrier (in kJ/mol, at 22 °C)

	K^+	Na^+	Ca^{2+}
f'_{out}	$2{\cdot}5 \times 10^9$	$2{\cdot}0 \times 10^9$	$4{\cdot}0 \times 10^9$
E_{01}	3·68	3·91	3·21
k'_{out}	$7{\cdot}9 \times 10^6$	$4{\cdot}1 \times 10^6$	$1{\cdot}9 \times 10^5$
E_{10}	14·05	14·7	17·77
k'_{in}	$7{\cdot}3 \times 10^7$	$4{\cdot}5 \times 10^7$	$2{\cdot}3 \times 10^6$
U_{01}	11·82	12·31	15·28
f'_{in}	$2{\cdot}3 \times 10^{10}$	$2{\cdot}2 \times 10^{10}$	$4{\cdot}7 \times 10^{10}$
U_{10}	1·47	1·51	0·75

As shown in Fig. 6*B–E*, these parameters account quite satisfactorily for the experimental observations, thus supporting the qualitative interpretation of cation conduction through the SA channel of the frog oocyte given above. The inward currents in particular could be exactly reconstructed. Concerning outward current, the model, as it is, predicts outward rectification when the membrane is strongly depolarized. We did not observe such rectification in the voltage range investigated; however, it is likely that the actual situation inside the oocyte may not reflect exactly that which we have assumed for simplicity. Mg^{2+} for example could exert a blocking effect on the outward currents (acting from inside), by analogy with that recently observed for the inwardly rectifying channel of heart muscle by Matsuda, Saigusa & Irisawa (1987). The above analysis not only defines the possible energy profile of the SA channel in the frog oocyte, but provides a precise interpretation of the inhibitory effect of Ca^{2+} on conduction of K^+ or Na^+ through the channel. From the rate constants in Table 2, the dissociation constant of the binding site towards the outside

$$K'_{D,X} = \frac{k'_{out,X}}{f'_{out,X}},$$

can be estimated. It represents the outside concentration of ion X at which the active site would have a probability 0·5 of being occupied, considering only transitions across the outer barrier in the absence of electric field across the membrane. The average occupancy time

$$\tau'_X = \frac{1}{k'_{in,X} + k'_{out,X}},$$

(Colquhoun & Hawkes, 1983) can also be estimated. From these equations, we find that Ca^{2+} presents a much smaller dissociation constant (50 μM) and much longer

occupancy time (400 ns) than Na^+ (2 mM and 20 ns respectively) or K^+ (3·2 mM and 12 ns respectively). In other words, the binding site of the SA channel in the frog oocyte displays more 'affinity' for Ca^{2+} than for Na^+ and K^+, and this fully explains the difference in conductance ('selectivity by affinity' in the sense of Eisenman & Horn, 1983) experienced by each cation. In the presence of external Ca^{2+} the channel occupancy is expected to increase, and the inward flow of Na^+ or K^+ will be competitively inhibited. The channel selectivity for the two monovalent cations will also be masked.

Both the dissociation constants and average occupancy times are predicted by the model to be voltage-dependent, exponentially decreasing with hyperpolarizing membrane potential. This could be related to the evident reduction in $K_{m,x}$ we constantly observed in the current–concentration experiments when membrane patches were hyperpolarized (see Table 1).

Possible functional role of the stretch-activated channel in the frog oocyte

There are many possible roles for the stretch-activated channel described here. When physiological saline is present outside, as it is when the oocyte lies in the ovary, channel activation by pressure (either positive or negative) will determine a net inward ion flux at the cell resting potential, and osmotic pressure should increase inside. This might represent a feed-back mechanism to resist compression exerted by neighbouring oocytes.

One could also speculate that the SA channel would be useful in the mature egg cell, provided that this channel is still present after maturation, which is known to involve dramatic changes in membrane conductances (Taglietti *et al.* 1984). The pond water in which frog egg cells are laid is in fact a very dilute solution, and the activation of the SA channel in this case would produce a net outward ion flux, thus possibly contributing to osmoregulation. However, consistent increase in cell volume and therefore in membrane stretch is effectively impaired in the ripe eggs by the presence of a thick and sturdy jelly coat. The channel could also have a role in fertilization, when egg membrane is stretched by the fertilizing sperm.

It has also to be considered that oocytes are cells with a highly de-repressed genome, with plasma membranes containing a variety of channels without any apparent usefulness as physiological tools. For example, amphibian oocytes are provided with receptors for acetylcholine (Toselli, Simoncini, Taglietti & Tanzi, 1985) and catecholamines (Kusano, Miledi & Stinnakre, 1982). The SA channel could represent here the precursor of the mechanoelectrical transducer which acts as stretch sensor in the mechanoreceptors of the adult organism; however its very high density argues against the possibility that it plays an aspecific role in the frog oocyte.

We are grateful to Dr Sergio Masetto (Institute of General Physiology, University of Pavia, Italy) who performed some useful experiments and prepared most of the iconography. This work was supported in part by grants of the Italian Ministry of Education (M.P.I.) and by the Italian Research Council (C.N.R.).

REFERENCES

ALMERS, W. & MCCLESKEY, E. W. (1984). Non-selective conductance in Ca-channels of frog muscle: calcium selectivity in a single pore. *Journal of Physiology* **353**, 585–608.

BEZANILLA, F. (1985). A high capacity data recording device based on a digital audio processor and a video cassette recorder. *Biophysical Journal* **47**, 437–442.

COLQUHOUN, D. & HAWKES, A. G. (1983). The principles of the stochastic interpretation of ion-channel mechanisms. In *Single-Channel Recording*, ed. SAKMANN, B. & NEHER, E., pp. 135–175. New York: Plenum Press.

COOPER, K. E., TANG, J. M., REE, J. L. & EISENBERG, R. S. (1986). A cation channel in frog lens epithelia responsive to pressure and calcium. *Journal of Membrane Biology* **93**, 259–269.

DUMONT, J. N. (1972). Oogenesis in *Xenopus laevis*: stages of oocyte development in laboratory maintained animals. *Journal of Morphology* **136**, 153–180.

DRAPER, N. & SMITH, H. (1980). *Applied Regression Analysis*. New York: John Wiley & Sons Inc.

EISENMAN, G. & HORN, R. (1983). Ionic selectivity revisited. The role of kinetic and equilibrium processes in ion permeation through channels. *Journal of Membrane Biology* **76**, 197–225.

EYRING, H. & EYRING, E. M. (1963). *Modern Chemical Kinetics*, chap. 4. New York: Reinhold Comp.

FALKE, L., EDWARDS, K. L., PICKARD, B. G. & MISLER, S. (1987). Stretch-activated anion channel in cultured tobacco cells. *Biophysical Journal* **51**, 251a.

FATT, P. & GINSBORG, B. L. (1958). The ionic requirements for the production of action potentials in crustacean muscle fibres. *Journal of Physiology* **142**, 516–543.

GUHARAY, F. & SACHS, F. (1984). Stretch-activated single ion channel currents in tissue-cultured embryonic chick skeletal muscle. *Journal of Physiology* **352**, 685–701.

GUHARAY, F. & SACHS, F. (1985). Mechanotransducer ion channels in chick skeletal muscle: the effects of extracellular pH. *Journal of Physiology* **363**, 119–134.

GUSTIN, M. C., ZHOU, X. L., MARTINAC, B., CULBERTSON, M. R. & KUNG, C. (1987). Stretch-activated cation channel in yeast. *Biophysical Journal* **51**, 251a.

HAMILL, O. P. (1983). Potassium and chloride channels in red blood cells. In *Single-Channel Recording*, ed. SAKMANN, B. & NEHER, E., pp. 451–471. New York: Plenum Press.

HAMILL, O. P., MARTY, A., NEHER, E., SAKMANN, B. & SIGWORTH, F. J. (1981). Improved patch-clamp techniques for high-resolution current recording from cells and cell-free membrane patches. *Pflügers Archiv* **391**, 85–100.

HILLE, B. (1975). Ionic selectivity of Na and K channels of nerve membranes. In *Membranes*, vol. 3, ed. EISENMAN, G., pp. 255–323. New York: Marcel Dekker.

HILLE, B. (1984). *Ionic Channels in Excitable Membranes*. Sunderland, MA, U.S.A.: Sinauer Associates Inc.

KUSANO, K., MILEDI, R. & STINNAKRE, J. (1982). Cholinergic and catecholaminergic receptors in the *Xenopus* oocyte membrane. *Journal of Physiology* **328**, 143–170.

LANSMAN, J. B., HALLAM, T. J. & RINK, T. J. (1987). Single stretch-activated ion channels in vascular endothelial cells as mechanotransducers? *Nature* **325**, 811–813.

LAUGER, P. (1973). Ion transport through pores. A rate theory analysis. *Biochimica et biophysica acta* **311**, 423–441.

LEWIS, C. A. & STEVENS, C. F. (1979). Mechanism of ion permeation through channels in a postsynaptic membrane. In *Membrane Transport Processes*, vol. 3, ed. STEVENS, C. F. & TSIEN, R. W., pp. 133–151. New York: Raven Press.

LEWIS, C. A. (1979). The ion concentration dependence of the reversal potential and single channel conductance of ion channels at the frog neuromuscular junction. *Journal of Physiology* **286**, 417–445.

MATSUDA, H., SAIGUSA, A. & IRISAWA, H. (1987). Ohmic conductance through the inwardly rectifying K channel and blocking by internal Mg^{2+}. *Nature* **325**, 156–159.

METHFESSEL, C., WEITZMANN, V., TAKAHASHI, T., MISHINA, M., NUMA, S. & SAKMANN, B. (1986). Patch-clamp measurements on *Xenopus laevis* oocyte: currents through endogenus channels and implanted acetylcholine receptor and sodium channels. *Pflügers Archiv* **407**, 577–588.

TAGLIETTI, V., TANZI, F., ROMERO, R. & SIMONCINI, L. (1984). Maturation involves suppression of voltage-gated currents in the frog oocyte. *Journal of Cellular Physiology* **121**, 576–588.

TOSELLI, N., SIMONCINI, L., TAGLIETTI, V. & TANZI, F. (1985). Acetylcholine-induced currents at plasma membrane of the frog oocyte. *Neuroscience Letters* **54**, 179–184.

URBAN, B. W. & HLADKY, D. A. (1979). Ion transport in the simplest single file pore. *Biochimica et biophysica acta* **554**, 410–429.

WOODBURY, J. W. (1971). Eyring rate theory model of the current–voltage relationships of ion channels in excitable membranes. In *Chemical Dynamics. Papers in Honour of H. Eyring*, pp. 601–617. New York: John Wiley & Sons Inc.

YANG, X. C., GUHARAY, I. & SACHS, F. (1986). Mechanotransducing ion channels: ionic selectivity and coupling to viscoelastic elements of the cytoskeleton. *Biophysical Journal* **49**, 373a.